Push–Pull Extrusion: A New Approach for the Solid-State Deformation Illustrated with High Density Polyethylene

TOSHIO SHIMADA, ANAGNOSTIS E. ZACHARIADES, MICHAEL P. C. WATTS, and ROGER S. PORTER, *Polymer Science and Engineering Department, Materials Research Laboratory, University of Massachusetts, Amherst, Massachusetts 01003*

Synopsis

The crystalline state deformation of high density polyethylene has been examined at an extrusion draw ratio of 30 over a range of temperatures and pressures. The experiments involve combined pushing (extrusion) and pulling through a conical die. The pressure dependence of the extrusion rate through conical dies is given by a logarithmic relation and the temperature dependence by an activation energy of ~95 kcal/mole. An equation established for the total applied force linearly relates the pulling and extrusion pressure components and represents a force balance at the die entrance and exit. Steady-state extrusion, with or without pulling, was feasible in a pressure range beyond which fractures occurred owing to strain rate and shear or tensile failure. Under some circumstances the extrusion rate was increased by ten times. The mechanical properties and mode of deformation were not affected by pull load and fibers with a tensile modulus of 55 GPa were produced at $T < 110°C$.

INTRODUCTION

Thermoplastics with a high tensile modulus have been obtained recently by introducing a high degree of chain orientation and by extension by solid-state extrusion[1] and drawing.[2]

In our laboratory, highly oriented states of high density polyethylene have been achieved by crystallization from the melt under combined orientation and pressure and later by deformation of preformed semicrystalline structures through a confining geometry at a sensitive choice of extrusion conditions.[3–5] This latter method is efficient in producing ultraoriented polyethylene extrudates, but operates only at slow extrusion rates. This limitation is partially overcome by the development of solid-state coextrusion.[6–8] This technique has produced continuous lengths of films and filaments for several polymers and for high-density polyethylenes of extrusion draw ratio (EDR) >30 at higher rates and at moderate pressures.

Pulltrusion processing[9] is common in metals and polymer composites. Correspondingly, the extrusion process used in this laboratory has potential over conventional drawing in that the polymer may be extruded under a combined push force and pull load on the emerging extrudate. Results indicate that the two stress modes may be interrelated, resulting in enhanced extrusion rates. Moreover, sizable tensile forces can be applied since the extrusion process produces high-modulus HDPE.

The object of this study is thus to investigate the effect of pulling loads on the

Journal of Applied Polymer Science, Vol. 26, 1309–1326 (1981)

0021-8995/81/041309-18$01.80

extrusion rate and processing conditions in the continuous production of ultraoriented (EDR > 30) high density polyethylene. In addition, the operation of a "push–pull" deformation mode provides the possibility of decoupling and interrelating the effects of pressure and the undercooling of crystal melting.

EXPERIMENTAL

Billets of high density polyethylene (DuPont Alathon 7050 $\overline{M}_w$ = 59,000; $\overline{M}_n$ = 19,900) were prepared void-free by compression under vacuum in an apparatus especially designed for this purpose.[10] The molded billets, ~7 cm long and 0.95 in diam, were subsequently split longitudinally in two halves and imprinted with a lateral pattern of lines which were 1 mm apart, to observe the deformation mode on extrusion [Fig. 1(a)]. The two marked halves were reassembled and press fitted to the reservoir of an Instron Rheometer. After equilibration at the desired extrusion temperature, pressure was applied and the polymer extruded through a conical brass die with a 20° entrance angle and an EDR of 30. The EDR is defined as the ratio of the inlet (0.95 cm diam) to the outlet (capillary) cross section areas of the die. Therefore, the extrusion was performed under the force of the ram only until extrudates of constant EDR = 30 were obtained in steady state. Thereupon, loads of different weights were attached on the extrudates through the pulley system depicted in Figure 1(b). The extrudate was mounted to clamp (a) and through pulleys (b) and (c) was attached to weight (e). Pulley (c) was equipped with a gear disk which would engage to a similar disk of the potentiometer (d) that was connected to a recorder. Thus, it was possible to observe the variation of extrusion rate with pulling force. Alternatively, the extrusion rate under the ram pressure was only measured with a cathetometer.

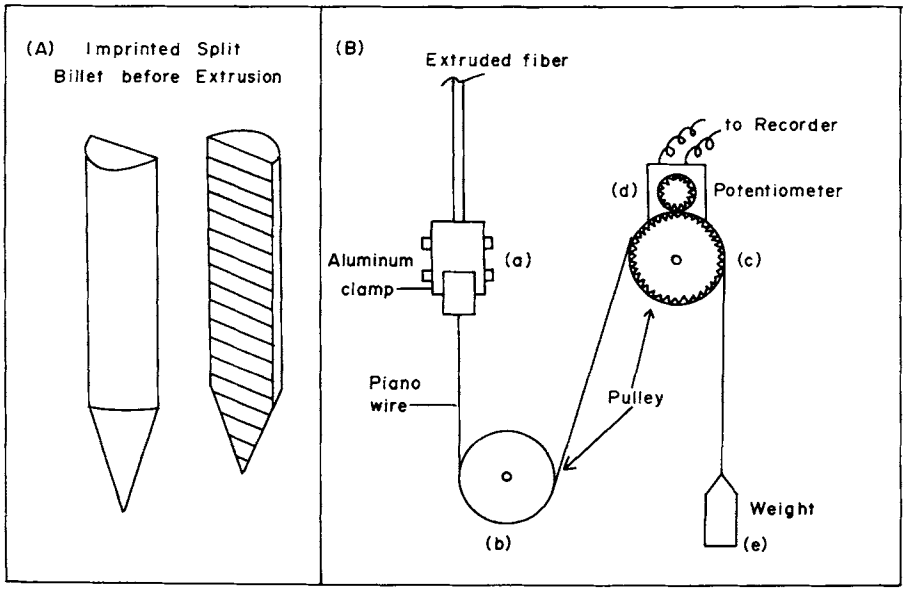

Fig. 1. (a) Imprinted split billet before extrusion; (b) pulley system for application of loads of different weights.

The stress–strain curves for the extrudates were measured at ambient and 120°C using an Instron environment chamber, on an Instron testing instrument, model TTM. The strain was measured at a strain rate of 6.5×10^{-5} sec^{-1}, and the modulus determined by the tangent to the stress–strain curve at 0.1% strain.

RESULTS AND DISCUSSION

Extrusion Without Pull Load

The variation of extrusion rate with extrusion pressure alone and temperature was first studied for steady-state extrusion at EDR = 30. Figure 2 shows that rate increases nonlinearly with extrusion pressure at various temperatures. Similarly, Figure 3 shows the rates also increase nonlinearly with temperature at the extrusion pressures indicated. Figure 4 shows that the extrusion rate with respect to the applied extrusion pressure is given by the equation

$$ln(ER) = k(P_A - P_0) \tag{1}$$

where ER is the extrusion rate, P_A the applied extrusion pressure, and P_0 and k are constants at a given temperature. This simple dependence of $ln(ER)$ on extrusion pressure has been observed previously by Mead and Porter[11] and is consistent with the Eyring yield criteria.[12] The temperature dependence of extrusion rate is given by the simple activation energy equation,

$$lnER = k' - \frac{\Delta H}{RT_E} \tag{2}$$

where T_E is the extrusion temperature and k' a constant. An activation energy plot is shown in Figure 4 and indicates a discontinuity at 105°C. This discontinuity, also observed by Mead and Porter,[11] was related to the α transition ob-

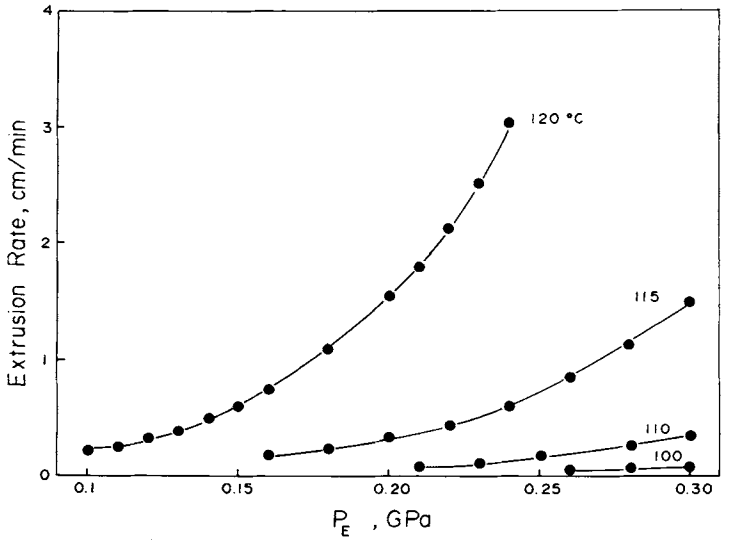

Fig. 2. Variation of extrusion rate with extrusion pressure at various temperatures for steady-state extrusion at EDR = 30.

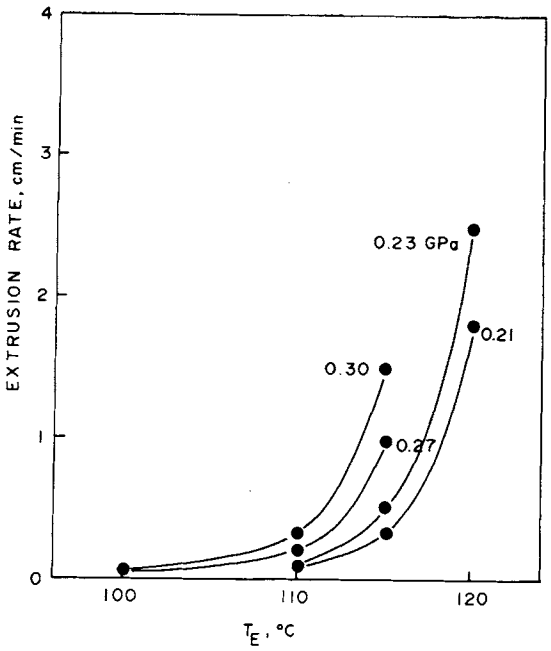

Fig. 3. Variation of extrusion rate with extrusion temperature at various pressures for steady-state extrusion at EDR = 30.

served in dynamic mechanical data with polyethylene. However, our data in the lower temperature region ($T < 110°C$) are not sufficient to indicate the dependence of the activation energy on the temperature range. Table I lists values for the constant k in eq. (1) at different temperatures and the activation energy in eq. (2) for different extrusion pressures.

Limits of Extrudability

Steady-state extrusion of transparent filaments, free of imperfections, at EDR = 30 without the effect of a pull load was possible when $P_A > P_{FL}$, where P_A is the extrusion pressure and P_{FL} represents the extrusion pressure limit below which onset of fracture occurs. At the pressure limit $P_{FL} = 0.12$ GPa the extrusion rate was 0.35 cm/min, below which fracture ensued at 120°C. We designate the fracture observed at $P_A < P_{FL}$ Fracture I, and believe that it associates with the strain rate of the deformation process. At extrusion pressures $P_A > P_{FL}$, e.g., $P_A = 0.13$ GPa ($ER = \sim 0.4$ cm/min), no fracture was observed and, upon application of tensile loads, the extrusion rate increases as will be described subsequently. Once below the 0.12 GPa limit, however, fracture developed at an angle ~30° to the extrusion direction from the outside to the center of the fiber, and, at $P_A = 0.08$ GPa, fracture was so severe that it had penetrated diagonally across the extrudate. Figure 5 illustrates the extent of fracture in the vicinity of the extrusion pressure limit, P_{FL}, at the same extrusion temperature (120°C) and at EDR = 30.

The occurrence of Fracture I at the same critical strain rate was also observed during the extrusion of fibers of lower EDR at the same extrusion temperature

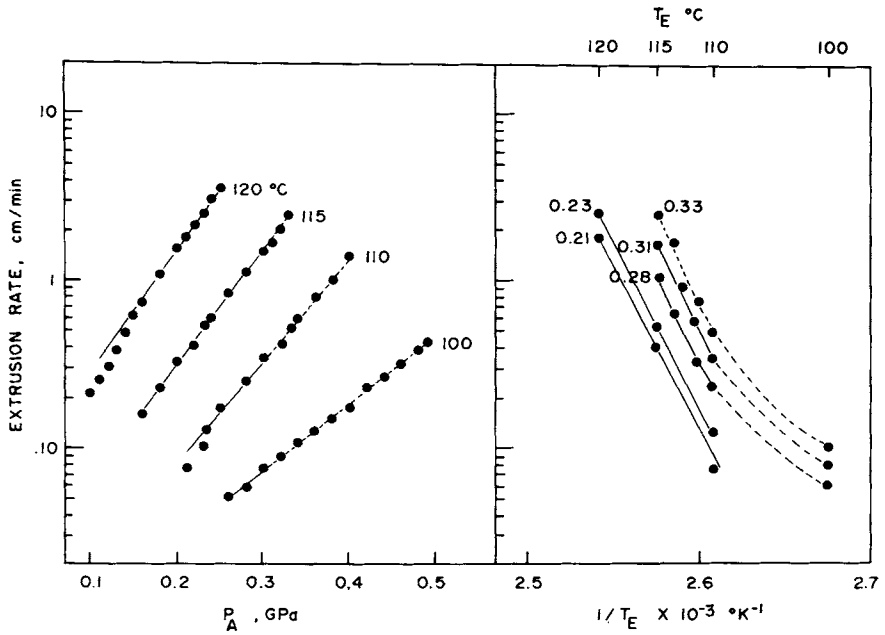

Fig. 4. Logarithmic plots of extrusion rate with (a) extrusion pressure and (b) extrusion temperature. Dashed lines represent data obtained under combined effects of extrusion pressure and pull load.

(120°C) and lower extrusion pressures. Thus, fibers of EDR 20, 23, 26, and 30 obtained at P_A = 0.07, 0.09, 0.11, and ~0.12 GPa, respectively, fractured in the same manner as discussed previously and, remarkably in all cases, at a constant rate 0.30 cm/min. However, Fracture I ensued at a lower strain rate when the extrusion temperature was lower. Thus, for fibers of EDR = 30 obtained at 115 and 110°C, the fracture occurred at 0.2 and 0.1 cm/min, respectively. Stick–slip failure occurred when excessive extrusion pressure was applied or changed suddenly. In this case, the extrudate fractured spirally along the extrusion direction.

Effect of Pull Load

It was discussed in the previous section that the equation $ln\ ER = k(P_A - P_0)$ describes the variation of extrusion rate with extrusion pressure. Without the influence of a pulling load, the applied pressure $P_A \equiv$ extrusion pressure P_E. In the presence of a pull load L, however, the applied pressure

$$P_A = f(P_E, P_L) \tag{3}$$

TABLE I

Values for Constant k in Eq. (1)		Values for the Activation Energy in Eq. (2)	
T_E°C	k(cm/min GPa)	P_E, Gpa	ΔH kcal/°K mole
120	7.22	0.21	89.7
115	6.91	0.23	90.6
110	6.24	0.27	92.3
100	4.13	0.30	95.6
		0.33	98.8

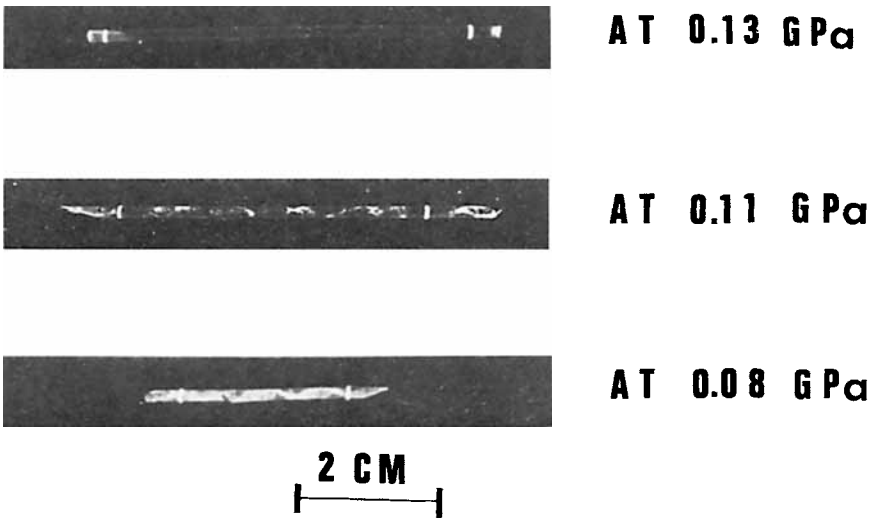

Fig. 5. Fracture I in vicinity of low pressure limit P_{FL} at 120°C. At 0.13 GPa, no fracture observed; at $P_A < 0.12$ GPa, fracture developed.

where P_E is the extrusion pressure and P_L is the pressure due to the attached load, L, on the emerging extrudate. The variation of extrusion rate with the two pressure components for a series of steady-state extrusions at EDR = 30 and at 120°C is shown in Figure 6. The extrusion pressures are indicated at the upper section of the figure, whereas the pressures owing to the applied loads are shown on the abscissa axis. The extrusion rate increased substantially with the pressure exerted by the attached loads, especially in the lower range of the extrusion pressures, e.g., 0.17–0.13, where the rate enhancement was up to tenfold.

The relation between P_E and P_L was established from Figure 6 by plotting the corresponding values of the two components versus each other at constant extrusion rate. A series of plots of P_E vs. P_L is shown in Figure 7. P_E decreases linearly as P_L increases. The two parameters are related by the equation

$$P_E = \lambda P_L \tag{4}$$

The proportionality constant λ can be obtained from the slope of the P_H vs. P_L plots and is independent of the extrusion rate. The calculated average λ value was 2.9 ± 0.2. Therefore, eq. (3) can thus be transformed to

$$P_A = P_E + \lambda P_L \tag{5}$$

Extrudability Limits

Like with the extrusions under the effect of the extrusion pressure alone, it was found that steady-state extrusion at EDR = 30 and at 120°C under the combined effects of the extrusion pressure and pull load was possible in the pressure range:

$$P_{FL} \equiv 0.12 \text{ GPa} < P_A = P_E + \lambda P_L < P_{FU} \tag{6}$$

The terms P_{FL} and P_{FU} denote the lowest and highest applied $(P_E + \lambda P_L)$ pressure limits beyond which onset of fracture occurs. Again, the lower pressure

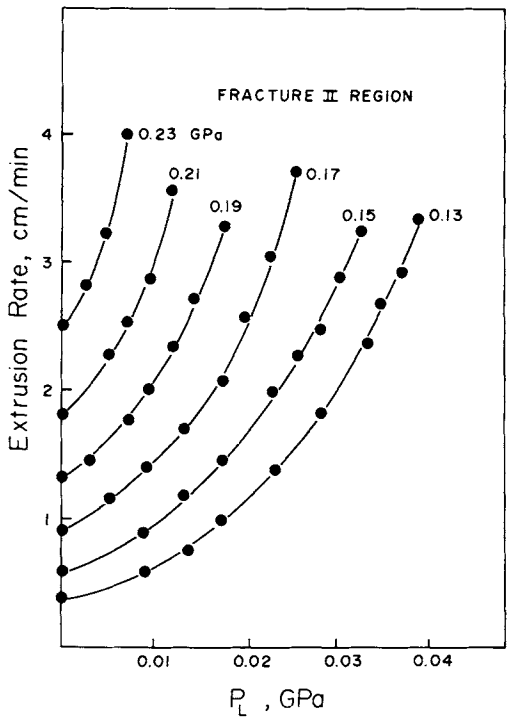

Fig. 6. Variation of extrusion rate with pull load for steady-state extrusion at EDR = 30, 120°C under various extrusion pressures.

limit P_{FL} is insensitive to the nature of the force, i.e., pull or push, and depends solely on the extrusion rate and consequently the strain rate of the deformation process.

P_{FU} is a different kind of fracture, designated Fracture II, and is attributed to tensile failure. As shown in Figure 7, the relation $P_E = \lambda P_L$ also holds at the Fracture II region and the proportionality constant, $\lambda = 2.9$, is in agreement with the values obtained from P_E vs. P_L plots at constant rate. From the relation between push and pull forces, the pressure at the base of the conical part of the die may be calculated (~0.07 GPa). This is similar to the tensile strength of the extrudate (0.04 GPa) at the extrusion temperature. Stick–slip failure occurred similarly to the extrusions under the extrusion pressure alone with sudden changes in total applied pressure and/or large extrusion pressure.[13]

Effect of Temperature

The effect of pulling upon extrusion was examined at different extrusion temperatures and at constant extrusion pressure. Figure 8 shows the variation of extrusion rate with pull load at extrusion pressure 0.23 GPa at the temperatures indicated for steady-state extrusions at EDR = 30. Although Fracture I was not observed with fibers extruded at 120, 115, and 110°C under 0.23 GPa, it occurred with fibers extruded at 100 and 90°C when the pull load, P_L, was smaller than 0.01 GPa (ER = ~0.05 cm/min) and 0.07 GPa (ER = ~0.01 cm/min), respectively. This change in rate with temperature for the onset of Fracture I further supports the idea that this type of fracture is strain rate dependent.

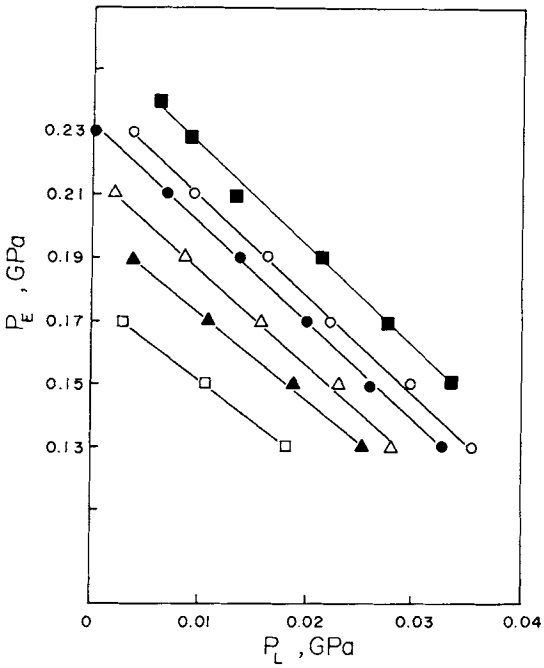

Fig. 7. Variation of extrusion pressure with applied load for steady-state extrusion at 120°C and EDR = 30 at rates: ○, 30; ●, 2.5; △, 2.0, ▲, 1.5; □, 1.0 cm/min; and in region of tensile failure, ■.

Superposition of Data

It is interesting to observe that the extrusion rate curves illustrated in Figures 2 and 8, and obtained without and with the effect of pull load at different extrusion temperatures, are superimposable. The rate data from the two figures have been replotted in Figure 9 against the applied pressure. The solid lines denote the rate variation at the temperatures indicated with the extrusion pressure alone; the dashed lines show the variation of the rate with the extrusion pressure plus pull load. On the left of the solid line perpendicular to the abscissa axis, $P_A = P_E$ (from Fig. 2) and on the right $P_A = P_E + \lambda P_L$ (from Fig. 8).

A similar plot of superimposable extrusion rate data obtained with and without pull load and at constant temperature in Figures 2 and 6 is depicted in Figure 10. These plots indicate that, in a push–pull extrusion process, forces up to the tensile fracture of the material can be applied so that the material can be obtained in a continuous process at the maximum draw ratio at a faster rate and under reduced extrusion pressure.

Effect of Pull Load on Modulus and Mode of Deformation

The tensile moduli for fibers extruded at different combinations of P_E and P_L and extrusion temperatures were measured at room temperature. Figure 11 shows that the modulus did not change with varying the P_E and P_L pressure components, but increased steeply as the extrusion temperature decreased below 110°C.

A study of the deformation profiles during extrusion with and without pulling indicated that the mode of deformation is not affected. Figure 12 illustrates

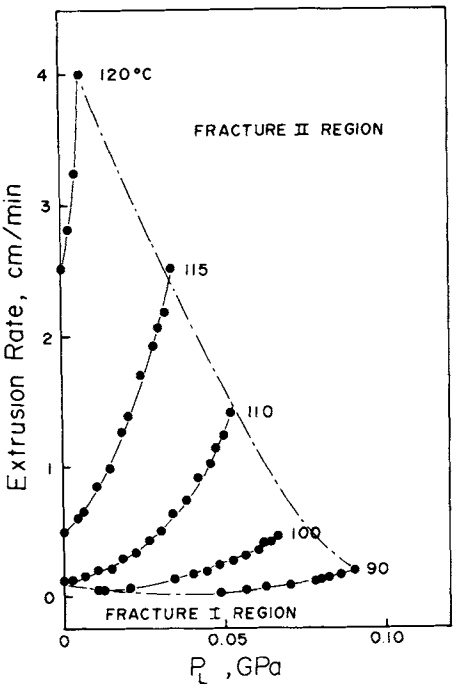

Fig. 8. Variation of extrusion rate with pull load at extrusion pressure 0.23 GPa and various extrusion temperatures.

the deformation profiles for an extrudate of (A) varying EDR, and of extrudates of constant EDR = 30 obtained (B) without and (C) with pulling.

Analysis

These results have highlighted some new features of solid-state extrusion and lead to a new model of the extrusion process as reported in the Appendix. The key conclusions that explain the push–pull extrusion data will be summarized here.

The observation that push and pull forces are additive through a constant λ confirms that there is a pressure drop across the die. It follows that the pressure applied to the polymer at the die exit $[P^*(\epsilon_0)]$, due to an extrusion pressure of P_E, will be given by

$$P^*(\epsilon_0) = \frac{P_E}{\lambda(\epsilon_0)} \tag{7}$$

where $\lambda(\epsilon_0)$ is the measured constant λ and ϵ_0 is the true strain of the die equal to ln(EDR).

For analysis, the mechanical properties of the polymer in the die are assumed to follow the stress–strain curve in tension obtained at the extrusion temperature and atmospheric pressure and at *the same strain rate as the extrusion.*

The extrusion pressure causes the polymer to yield and in the process performs work. The work is given by the area under the stress–strain curve. These polymers show very large strain hardening during extrusion[14] and, therefore,

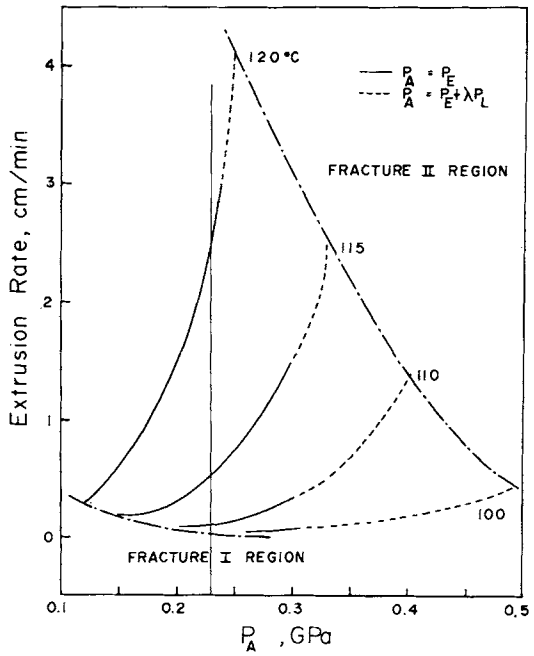

Fig. 9. Superposition of rate data plotted in Figs. 2, 8. —, variation of extrusion rate with extrusion pressure, P_E; ---, represent rate variation with total applied pressure, $P_A (P_A = P_E + \lambda P_L)$.

the significant part of the extrusion occurs at higher strains, i.e., at the base of the die cone. The variation of applied pressure with strain is less than that of stress with strain; therefore, the applied pressure may be assumed, for simplicity, to be constant and equal to the value at the base of the die cone. As a result, the extrusion pressure is given by the sum of the yield stress at strain ϵ_0 and the area under the stress–strain curve of the yielded polymer multiplied by the factor relating the die entrance and exit pressures,

$$P_E + \lambda(\epsilon_0) P_0 = \lambda(\epsilon_0) \left[\int_0^{\epsilon_0} \sigma(\epsilon) d\epsilon + \sigma(\epsilon_0) \right] \tag{8}$$

At fracture, $\sigma(\epsilon_0)$ becomes the tensile strength σ_t and

$$\int_0^{\epsilon_0} \sigma(\epsilon) d\epsilon = P_0 + \frac{P_E}{\lambda(\epsilon_0)} - \sigma_t \tag{9}$$

where $P_0 + P_E/\lambda(\epsilon_0)$ is the total applied pressure at the base of the cone. The tensile data show that the work of deformation requires less than 50% of the extrusion pressure, i.e., a major fraction of the extrusion pressure is required to yield the material. Furthermore, eq. (8) shows that the parameter $\lambda(\epsilon_0)$ is major in determining the extrusion pressure.

The pressure balance theory shows that

$$\lambda(\epsilon_0) = \exp(B\epsilon_0) \tag{10}$$

where B is $\mu \cot\alpha$, μ is the coefficient of friction, and α is the die angle. Thus, if λ equals 3, B equals 0.3066, and hence μ is 0.05. The push–pull test thus allows

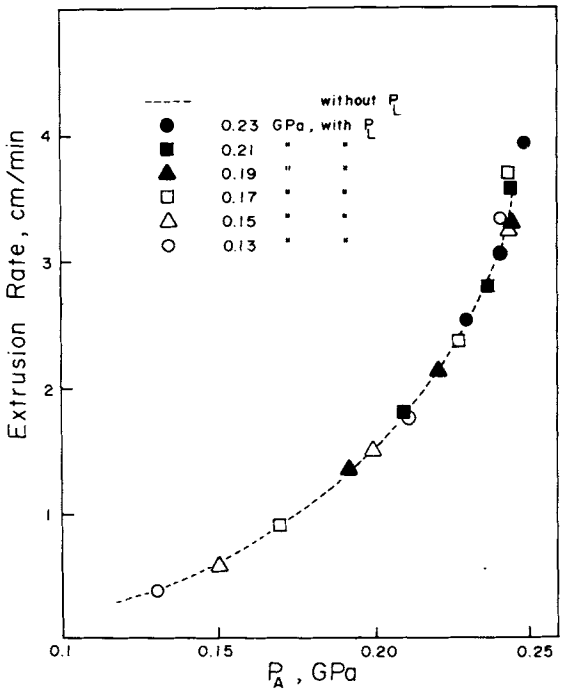

Fig. 10. Superposition of rate data plotted in Figs. 2 and 6.

an unambiguous measurement of μ that had previously only been found by curve fitting theories to extrusion rate data.[15] This analysis shows that $\lambda(\epsilon_0)$ and hence, P_E, could be reduced by lubrication and multistep extrusion, an important observation for the development of efficient extrusion. Finally, the push–pull test allows the contributions of friction and shear, that overlap in die angle studies, to be decoupled.[16]

It may be speculated that a primary effect of pressure involves elevation of melting point, i.e., increased undercooling, by pressure. The fact that pull and push are linearly additive and proportional to the logarithm of extrusion rate shows that the effect of pressure follows the Eyring yield mechanism, and hence undercooling is not a factor for this range. The mechanical properties of the extrudates are also not affected by extrusion pressure. This is further evidence that undercooling does not affect the load bearing components of the final morphology.

As illustrated earlier, the onset of fracture at low extrusion pressures ($P_A < P_{FL}$) occurs at a constant strain rate. This appears to be similar to the fracture at low elongations observed at low strain rates and/or high temperatures in elastomers, as seen in the fracture envelope. Smith[17] reviewed the strength of elastomers, suggesting that slow crack growth occurs from dissipation of stored elastic energy through viscoelastic processes. If the extrusion rate is sufficiently slow, the rate of crack growth is faster than the rate of deformation and the fracture (Fracture I) reported in the previous section occurs.

The push–pull process allows aspects of the solid-state extrusion process to be understood. Furthermore, it provides practical significance. Thus, the

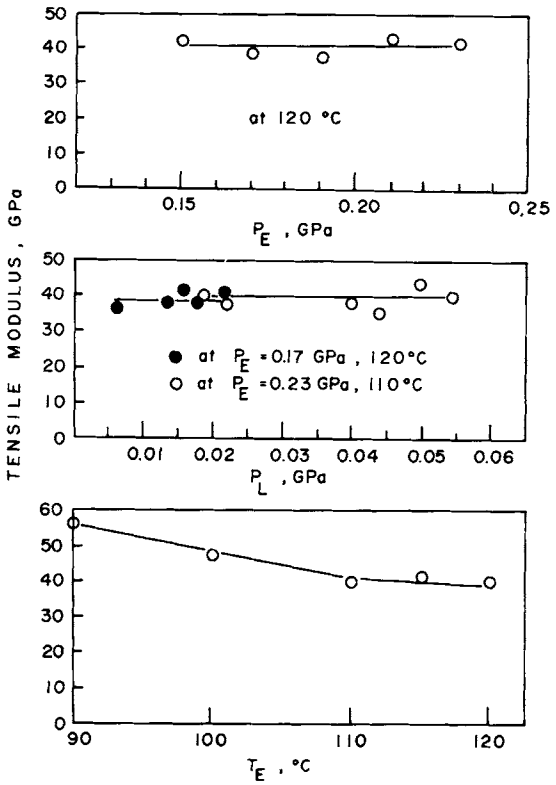

Fig. 11. Variation of tensile modulus for extruded fibers at EDR = 30 with (a) extrusion pressure, (b) pull load, (c) extrusion temperature.

maximum pressure that may be applied for extrusion of polyethylene under the extrusion conditions of this study is limited to 0.23 GPa because of stick–slip extrusion at higher pressures. This imposes a "process-dependent" restriction on the maximum extrusion rate and, consequently, on the maximum draw ratio that may be obtained at significant extrusion rates. In push–pull extrusion, however, forces up to the fracture strength may be applied; hence, the maximum extrusion rates and draw ratios up to the fracture strain may be obtained. This allows a substantial increase in the range of the extrusion process.[7]

CONCLUSIONS

The effect of pulling on solid-state extrusion has been investigated for HDPE at EDR = 30 and at a series of temperatures and pressures. The principal features observed experimentally can be summarized as follows:

(1) The extrusion rate (ER) with respect to the applied pressure ($P_A = P_E + \lambda P_L$) is given by eq. (1). $P_A = P_E + \lambda P_L$ was established experimentally and represents a hydrostatic balance of forces at the entrance and exit of the die.

(2) The temperature dependence of extrusion rate is given by the activation energy equation [eq. (2)] in which the activation energy is ~95 kcal/mole; below 110°C divergence from linearity is observed.

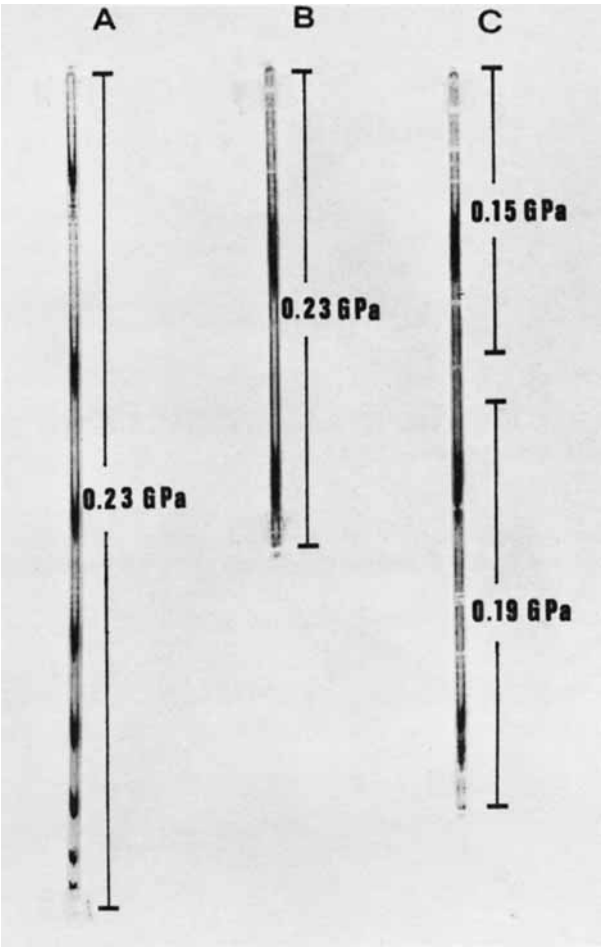

Fig. 12. Deformation profiles of extruded fibers with (c) and (b) pull load and of increasing EDR up to 30 (a) from bottom to top.

(3) Steady-state extrusion of HDPE fibers with or without pulling at an EDR = 30 and 120°C, free of imperfections, is feasible in the pressure range:

$$P_{FL} = 0.12 \text{ GPa} < P_A = P_E + \lambda P_L < P_{FU}$$

where P_{FL} and P_{FU} are temperature dependent; Fracture I is strain rate dependent; Fracture II is associated with tensile failure (at Fracture II the applied pressure equals the tensile strength of the polymer at the extrusion temperature); and stick–slip is caused by sudden changes in total applied pressure (P_A) and/or excessive extrusion pressure (P_E).

(4) The mechanical properties and mode of deformation are not affected by pull load. However, as a result of pulling the steady-state extrusion of HDPE fiber with increased modulus was possible at $T < 110$°C.

The authors express their appreciation to Dr. P. D. Griswold for his help and design of the original experiments and to the National Science Foundation for financial support.

APPENDIX A

An Analysis of the Extrusion Process

Results reported here allow an reassessment of the key features of the extrusion process. During extrusion an isotropic polymer is plastically deformed through a conical die under a pressure gradient to give an anisotropic extrudate.

The cross section of the die is shown in Figure A1(a), and the change in extrusion draw ratio [EDR = $(R_E/r)^2$] and true draw ratio [$\epsilon = 2ln(R_E/r)$][14] along the die cone in Figure A1(b), A1(c), respectively. Note that the strain is nonlinear with respect to die radius. In push–pull extrusion, the addition of the pull load to the extrudate allows the pressure drop across the die to be varied at constant extrusion pressure. Push and pull loads were found to be additive through a constant λ that was independent of the extrusion rate. The application of an extrusion pressure P_E has been shown to be equivalent to a pull load of P_E/λ at the die exit. Thus, there is a transmission of hydrostatic pressure across the die. It follows that the applied pressure must be changing across the die cone and λ is a function of strain ϵ_0. Therefore, $\lambda(\epsilon)$ at the die exit may be expressed by $\lambda(\epsilon_0)$ and the applied pressure at any strain ϵ as $P^*(\epsilon)$ by

$$P^*(\epsilon) = P_E/\lambda(\epsilon) \tag{A-1}$$

Theories of extrusion emphasize the following contributions to the resistance to extrusion. Pressure is required (a) to shear and elongate the polymer and (b) to overcome the die–polymer friction. A relation between entrance and exit pressure is given by the pressure balance model of Nakamura, Imada, and Takayanagi,[15] giving an expression for $\lambda(\epsilon)$ of

$$\lambda(\epsilon) = \exp(B\epsilon) \tag{A-2}$$

where B is $\mu \cot(\alpha)$. μ is the coefficient of friction and α the die half angle. Hence, pressure drop is seen to result from significant friction between the polymer and die. From $\lambda(\epsilon_0)$ found in the push–pull tests, $B = .3066$ and, hence, $\mu = 0.05$ (previously μ had only been found using curve fitting theories to extrusion rate data).

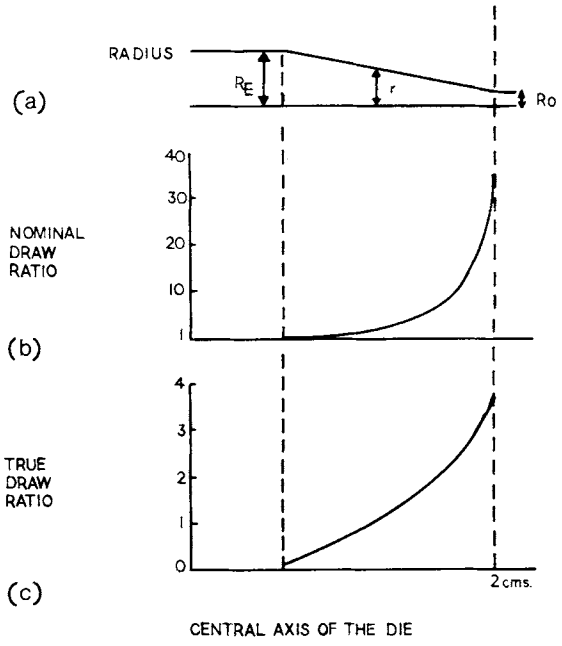

Fig. A1. Schematic cross section of die showing change in strain.

Using eq. (A-2), the change in applied pressure across the die may be calculated. Figure A2(a) shows the change in die radius with true draw ratio, with the entrance and exit regions also included for clarity [the "inverse" of Fig. A2(c)]. Figure A2(b) shows the change in applied pressure along the die. In section 1 there is a pressure drop due to a finite length of undeformed polymer and it is assumed to be negligible.[11] In section 2 the applied pressure $P^*(\epsilon)$ is

$$P^*(\epsilon) = P_E \exp(-B\epsilon) \tag{A-3}$$

Finally, at the die exit (section 3), the pressure is one atmosphere. It is important to note that the change in applied pressure along the die follows directly from the experimental observation of $\lambda(\epsilon_0)$ and assumes a function for $\lambda(\epsilon)$ [eq. (A-2)].

A measure of the mechanical properties of the polymer in the die is required. Near the limit of zero die angle, the plastic deformation should consist of pure elongation; as the die angle is increased, shear deformation increases as observed in flow profile studies.[18] With the die angle used here (α = 10°), the shear deformation can be neglected.[19] Any attempt to use the mechanical properties at atmospheric pressure to discuss the properties in the die is usually accompanied by the disclaimer that there is no knowledge of how pressure in the die affects the stress–strain properties of the polymer.[15] However, there is evidence from three different sources[11,20] that the relation between extrusion rate and pressure is given by the Eyring yield equation.[12] This relation has been applied to the drawing process[21] and the creep properties of oriented HDPE rods,[22] all at atmospheric pressure. This infers that effects such as melting point undercooling and increased hydrostatic pressure, leading to an increased yield stress, are not significant. It appears that the elongation properties in the die are given by the true stress–strain curve at atmospheric pressure at the same strain rate as the extrusion. It is important to note that this differs from the definition used by Nakamura, Imada, and Takayanagi.[15] They considered that a "critical" pressure is required to start the extrusion. Subsequently, the Eyring yield relation was found to apply and clearly there is no "critical" pressure in a material showing a log extrusion rate–extrusion pressure relation. Therefore, the strain rate must be included in the definition of the stress–strain curve. Furthermore, the equations used here are *applicable to all extrusion rates* because the connection between extrusion rate and pressure is made through changes in the stress–strain curve at different strain rates.

During deformation in the die, the extrusion pressure must cause yield and perform work. Therefore, the actual pressure in the die will be given by

$$P(\epsilon) = P^*(\epsilon) - \sum_0^{\epsilon} W(\epsilon) \tag{A-4}$$

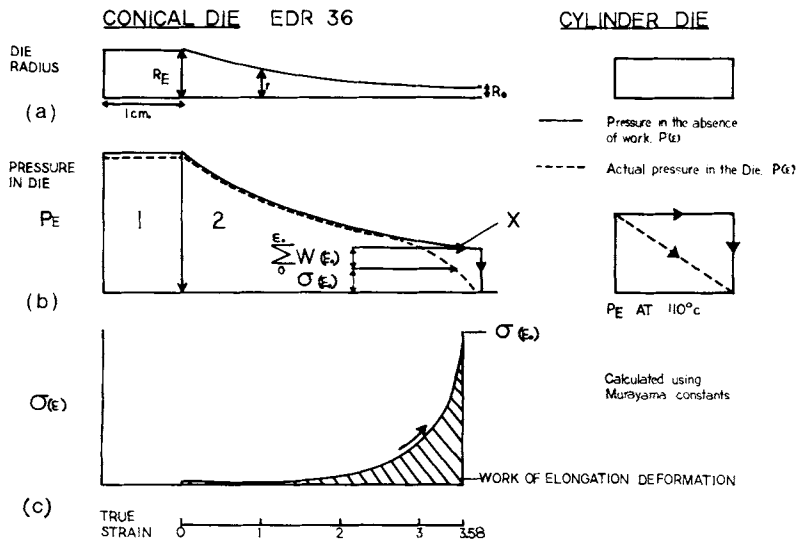

Fig. A2. Schematic showing pressure drop across die.

where $\sum_0^{\epsilon} W(\epsilon)$ is the work of deformation between 0 and ϵ calculated at strain ϵ. The strain at which the work is calculated must appear in the general expression $\sum W(\epsilon)$ because work is defined relative to the applied pressure and the applied pressure varies along the die. For example,

$$\sum_0^{\epsilon_0} W(0)$$

is the work of deformation between 0 and ϵ_0 calculated at strain 0, i.e., the die entrance. It is the work relative to the extrusion pressure.

To yield the material

$$P(\epsilon) \geqslant \sigma(\epsilon) \tag{A-5}$$

where $\sigma(\epsilon)$ is the true stress at strain ϵ at the strain rate of extrusion; this condition has not been included in previous theories.

The true stress strain curve for HDPE at 110°C may be calculated from the data of Murayama, Imada, and Takayanagi;[14] and is shown in Figure A2(c). Because of strain hardening, the condition in eq. (A-5) may be rewritten

$$P(\epsilon_0) = \sigma(\epsilon_0) \tag{A-6}$$

for the extrusion to proceed. Therefore, at the base of the die cone in a push–pull test, eq. (A-4) becomes:

$$P(\epsilon_0) = \frac{P_E}{\lambda(\epsilon_0)} + P_0 - \sum_0^{\epsilon_0} W(\epsilon_0)$$

and combining with eq. (A-6):

$$\sum_0^{\epsilon_0} W(\epsilon_0) = \frac{P_E}{\lambda(\epsilon_0)} + P_0 - \sigma(\epsilon_0). \tag{A-7}$$

At fracture, the yield stress becomes the tensile strength that can be measured by a conventional tensile test, at 120°C, σ_ϵ is 0.04 GPa and a comparison with the applied pressure at the base of the die $[P_E/\lambda(\epsilon_0) + P_0 = 0.07$ GPa] gives a measure of the work of deformation. Therefore, the measurements of the tensile failure show that of the total applied extrusion pressure, approximately 50% is required to stress the material and the rest is due to work. The addition of the boundary condition (A-6) and (A-7) is crucial for a correct description of the extrusion process.

The work of deformation is given in the pressure balance theory as:

$$\begin{aligned} P_E &= \int_0^{\epsilon_0} \sigma(\epsilon) \exp(B\epsilon) d\epsilon \\ &= \sum_0^{\epsilon_0} W(0) \text{ in this nomenclature.} \end{aligned} \tag{A-8}$$

$\Sigma_0^{\epsilon_0} W(0)$ is the work of deformation *calculated at the die entrance.* Note the absence of a term in $\sigma(\epsilon_0)$ outside the integral. The area under the stress–strain curve is modified by the term $\exp(B\epsilon)$ so that the yield stress at ϵ is considered relative to the pressure at ϵ. In the same way, to calculate the work at strain ϵ, $[\sum_0^{\epsilon} W(\epsilon)]$, a term must be added to allow for variations in pressure from $P^*(\epsilon)$. However, the polymer strain hardens so that the majority of the work done in getting to strain ϵ is done near strain ϵ. $\text{Exp}(B\epsilon)$ is a less sensitive function of ϵ than $\sigma(\epsilon)$, particularly at high strain, therefore variations in $P^*(\epsilon)$ may be ignored and

$$\sum_0^{\epsilon} W(\epsilon) = \int_0^{\epsilon} \sigma(\epsilon) d\epsilon \tag{A-9}$$

Using eqs. (A-4) and (A-9) and the example in Figure A3(c), the actual pressure profile $P(\epsilon)$ may be calculated in Figure A3(b). Note that the applied and actual pressure only diverge in the high strain region. Thus, the push–pull test allows the complete pressure profile to be drawn.

Combining eqs. (A-7) and (A-9), the pressure at the die exit is given by [see Fig. A2(b) where $P_0 = 0.0$]:

$$\frac{P_E}{\lambda(\epsilon_0)} + P_0 = \int_0^{\epsilon_0} \sigma(\epsilon) d\epsilon + \sigma(\epsilon_0) \tag{A-10}$$

and at the die entrance

$$P_E + \lambda(\epsilon_0) P_0 = \lambda(\epsilon_0) \left[\int_0^{\epsilon_0} \sigma(\epsilon_0) \right] \tag{A-11}$$

Eq. (A-11) simply says that the extrusion pressure equals the work and yields stress at the die exit multiplied by the constant relating exit pressures to entrance pressure. The significance of the experimentally measured parameter $\lambda(\epsilon_0)$ may be expressed as

$$P_E \propto \lambda(\epsilon_0)$$

Eq. (A-11) may be rewritten using the Nakamura expression for $\lambda(\epsilon)$ as

$$P_E + e^{(B\epsilon_0)}P_0 = e^{(B\epsilon_0)}\left[\int_0^{\epsilon_0}\sigma(\epsilon)d\epsilon + \sigma(\epsilon_0)\right] \tag{A-12}$$

where B is $\mu \cot\alpha$.

The extrusion pressure increases with increasing friction and strain in the die. The pressure drop due to friction will be minimized by the use of lubrication or hydrostatic extrusion and by multistep extrusion where the material is drawn from, say, EDR 0 → 10, then 10–20, then 20–30, etc., in a series of individual operations. Also the effectiveness of the addition of a pull load is reduced at the same time.

Using Eq. (A-11), the extrusion pressure and rate may be calculated from stress–strain data. Table AII shows data based on the stress–strain curve in Figure 14(c) obtained at 110°C on HDPE with a melt flow index of 9.2 and initial strain rate of $\simeq 0.004\ \text{sec}^{-1}$. The maximum extrusion pressure used is 0.23 GPa as the draw ratio will be 15–17 at an extrusion rate of 6 cm min^{-1}, consistent with other data from this laboratory.

Effect of Die Angle Variation

According to the pressure balance theory,[15] $\lambda(\epsilon)$ drops rapidly with half die angle α, hence, P_E also drops. This results from the increase in die surface area at low die angles. At higher die angles the pressure drop increases again because of increased shear deformation,[23] so a minimum in extrusion pressure at constant rate or a maximum in rate at constant pressure should be observed when there is significant friction. The latter has been observed by Perkins[19] in this laboratory, consistent with Nakamura's equations. Finally, eq. (A-12) may be generalized to account for shear and, thus, to give a complete description of extrusion. Most of the significant shear will occur near the die exit. Therefore,

$$P_E + e^{(B\epsilon_0)}P_0 = e^{(B\epsilon_0)}\left[\int_0^{\epsilon_0}\sigma(\epsilon)d\epsilon + \sigma(\epsilon_0) + S(\epsilon_0,\alpha)\right]$$

where S is the work of shear and shear yield at strain ϵ_0 and die angle α.

The key features of a model of the extrusion may be summarized. The mechanical properties of the polymer in the die are adequately given by the true stress–strain curve in tension obtained at the extrusion temperature and atmospheric pressure and at the same strain rate as the extrusion. Because of the large strain hardening in polymers, the "rate determining" step occurs near the base of the die cone. The pressure at the base of the die must be sufficient to cause yield and overcome the work of deformation that is given by the area under the stress–strain curve. The extrusion pressure is then related to the pressure at the base of the die by the proportionality factor $\lambda(\epsilon_0)$, that is a function of the die angle, strain, and friction. The push–pull tests allow an unambiguous measure of the friction coefficient and show that, for the method used here, friction is significant and must be included in any model of the extrusion process.

TABLE II
Data Based on Stress–Strain Curve in Fig. A2(c) for Extrusions at 120°C and through Conical Die with Tapered Angle of 20°

Nominal draw	12	24	36
True draw, EDR	2.48	3.28	3.58
$\sigma(\epsilon)$, GPa	0.034	0.112	0.275
$\int_0^{\epsilon}\sigma(\epsilon)d\epsilon$, GPa	0.029	0.071	0.128
$\lambda(\epsilon_0) = \exp(B\epsilon_0)$	2.1	2.6	3.0
P_E, GPa	0.13	0.48	1.2

References

1. K. Imada, T. Yamomoto, K. Shigematsu, and M. Takayanagi, *J. Mater. Sci.*, **6**, 537 (1971).
2. P. B. Bowden and R. F. Young, *J. Mater. Sci.*, **9**, 2034 (1974).
3. J. H. Southern and R. S. Porter, *J. Appl. Polym. Sci.*, **14**, 2305 (1970).
4. N. E. Weeks and R. S. Porter, *J. Polym. Sci., Part A2*, **12**, 635 (1974).
5. N. J. Capiati, S. Kojima, W. G. Perkins, and R. S. Porter, *J. Mater. Sci.*, **13**, 334 (1977).
6. P. D. Griswold, A. E. Zachariades, and R. S. Porter, *Polym. Eng. Sci.*, **18**, 861 (1978).
7. M. P. Watts, A. E. Zachariades, and R. S. Porter, 9th Biennial Polym. Symp., Key Biscayne, Fla., Nov. 1978.
8. T. Shimada, A. E. Zachariades, W. T. Mead, and R. S. Porter, *J. Crystal Growth*, accepted for publication.
9. *Modern Plastics Encyclopedia*, Vol. 55, no. 10A, McGraw-Hill, New York.
10. A. E. Zachariades, P. D. Griswold, and R. S. Porter, *Polym. Eng. Sci.* **19**, 6 (1979).
11. W. T. Mead and R. S. Porter, *J. Polym. Sci., Polym. Chem. Ed.*, accepted for publication.
12. H. Eyring, *J. Chem. Phys.*, **14**, 283 (1936).
13. J. A. Brydson, *Flow Properties of Polymer Melts*, Van Nostrand, New York, 1970.
14. S. Murayama, K. Imada, and M. Takayanagi, *Int. J. Polym. Mater.*, **6**, 211 (1979).
15. K. Nakamura, K. Imada, and M. Takayanagi, *Int. J. Polym. Mater.*, **2**, 71 (1972).
16. S. Murayama, K. Imada, and M. Takayanagi, *Int. J. Polym. Mater.*, **2**, 125 (1973).
17. T. L. Smith, *Polym. Eng. Sci.*, **17**, 3 (1973).
18. T. Kanamoto, A. E. Zachariades, and R. S. Porter, *Polymer J.*, **11**, 307, (1979).
19. W. G. Perkins, Ph.D. thesis, University of Massachusetts, Amherst, 1978.
20. C. J. Farrell and A. Keller, *J. Mater. Sci.*, **12**, 966 (1977).
21. G. Capaccio and I. M. Ward, *Polymer*, **16**, 239 (1975).
22. M. A. Wilding and I. M. Ward, *Polymer*, **19**, 969 (1978).
23. A. G. Kolbeck and D. R. Ullmann, *J. Polym. Sci., Polym. Phys. Ed.*, **15**, 27 (1977).

Received July 13, 1979
Accepted September 26, 1980